UCLA

UCLA Previously Published Works

Title

Aminodealkenylation: Ozonolysis and copper catalysis convert C(sp3)-C(sp2) bonds to C(sp3)-N bonds.

Permalink

https://escholarship.org/uc/item/4079v0qk

Journal

Science, 381(6660)

Authors

He, Zhiqi
Moreno, Jose
Swain, Manisha
et al.

Publication Date

2023-08-25

DOI

10.1126/science.adi4758

Peer reviewed

Aminodealkenylation: Ozonolysis and copper catalysis convert C(sp³)–C(sp²) bonds to C(sp³)–N bonds

Zhiqi He,

Jose Antonio Moreno,

Manisha Swain,

Jason Wu,

Ohyun Kwon[*]

Department of Chemistry and Biochemistry, University of California, Los Angeles, CA 90095-1569, USA.

Abstract

Great efforts have been directed toward alkene π bond amination. In contrast, analogous functionalization of the adjacent $C(sp^3)$–$C(sp^2)$ σ bonds is much rarer. Here we report how ozonolysis and copper catalysis under mild reaction conditions enable alkene $C(sp^3)$–$C(sp^2)$ σ bond–rupturing cross-coupling reactions for the construction of new $C(sp^3)$–N bonds. We have used this unconventional transformation for late-stage modification of hormones, pharmaceutical reagents, peptides, and nucleosides. Furthermore, we have coupled abundantly available terpenes and terpenoids with nitrogen nucleophiles to access artificial terpenoid alkaloids and complex chiral amines. In addition, we applied a commodity chemical, α-methylstyrene, as a methylation reagent to prepare methylated nucleosides directly from canonical nucleosides in one synthetic step. Our mechanistic investigation implicates an unusual copper ion pair cooperative process.

Editor's summary

Reactions that form carbon–nitrogen bonds most often target carbon centers that are either single bonded to a halogen or double bonded to oxygen or another carbon. He *et al.* present an alternative sequence that targets a carbon–carbon single bond adjacent to an olefin. Treatment of the allylic

[*]Corresponding author. ohyun@chem.ucla.edu.

SUPPLEMENTARY MATERIALS

science.org/doi/10.1126/science.adi4758

Materials and Methods

Supplementary Text

Figs. S1 to S47

Tables S1 to S7

Characterization Data

References (59–129)

View the article online

https://www.science.org/doi/10.1126/science.adi4758

carbon compound with ozone followed by copper catalysis formally displaces the pendant olefin with an amine. The reaction can introduce nitrogen into a wide variety of complex terpenes, among other compounds. —Jake S. Yeston

---

The importance of aliphatic amines and nitrogen heterocycles is evidenced by their wide representation in natural products, pharmaceuticals, agrochemicals, and other bioactive compounds (1). The increasing demand in medicinal research for more-complex three-dimensional architectures and optically active amines has driven efforts to develop diverse practical methods for $C(sp^3)$–N bond construction (2, 3). Conventionally, the electron-rich nature of amino nitrogen atoms renders them strong nucleophiles that can attack the polarized chemical bonds of alkyl halides, alcohol derivatives, and carbonyls, thereby forging new $C(sp^3)$–N bonds. Engaging ubiquitous and nonpolar C–C bonds in $C(sp^3)$–N bond construction is an intriguing strategy because such transformations can be used to modify molecular skeletons directly and, thereby, access conventionally challenging or inaccessible aliphatic amines (4–6). Classical methods for C–C bond amination, including the Lossen, Hofmann, Curtius, Beckmann, and Schmidt rearrangements, which typically rely on 1,2-migration of an alkyl or aryl group from carbon to nitrogen (Fig. 1A, reactions 1 and 2), have demonstrated their utility in the syntheses of bioactive molecules and in industrial manufacturing. For example, 5.5 million metric tons of caprolactam, a precursor to nylon 6, are produced annually through the Beckmann rearrangement of cyclohexanone oxime (7). Although these classical transformations are powerful methods for accessing nitrogen insertion products, the sources of the C–C bonds are limited mostly to ketones and carboxylic acids, and the sources of nitrogen atoms are limited to those that insert one N atom, leaving room for incorporation of alternative, perhaps more ubiquitous, chemical functionalities as the sources of both the C–C and C–N bonds.

In the past 5 years, several important advances have sought to address those limitations in the sources of both the C–C bonds and nitrogen atoms in C–C amination. The Jiao group employed the C–C bonds of alkylarenes, styrenes, and alkynylarenes in a Schmidt-type reaction, although the products were limited to anilines with new $C(sp^2)$–N bonds, owing to the preferred migration of the aryl group (Fig. 1A, reaction 3) (8–10). Fu, Hu, MacMillan, Martin, and colleagues disclosed deconstructive $C(sp^3)$–N couplings of carboxylic acid and ketone derivatives that overcame the limitation of 1,2-migration chemistry, providing methods to construct $C(sp^3)$–N bonds with various N-heteroarenes, amides, and anilines (Fig. 1A, reaction 4) (11–15). Despite these advances, there remains a huge scope for new sources of C–C bonds, beyond carbonyl compounds, for amination (16–20). In particular, developing methods to exploit a starting material's skeletal complexity to access chiral amine architectures would be highly desirable.

Alkenes are versatile functional groups that are abundant in natural products and industrial chemicals. In fact, C=C double bonds are the second most frequently encountered functional group in natural products (39.9%), exceeding ketone (15.9%) and carboxylic acid (10.6%) functionalities (21). Because chiral centers are common within natural products, we surmised that the alkene moieties in natural products might serve as ideal C–C bond amination precursors for constructing complex chiral amines from naturally occurring

chiral-pool molecules. Most methods for installing nitrogen groups to alkene motifs have focused on addition across the C–C π bond to produce peripheral amination products (Fig. 1B) (3). Conversely, the adjacent $C(sp^3)$–$C(sp^2)$ σ bonds have received less attention for C–N bond construction (Fig. 1C, top). We envisioned that a C–N bond coupling strategy involving unusual C–C bond disconnections would constitute a distinct paradigm for alkyl amine synthesis, with several implications. First, this strategy could access artificial terpenoid alkaloids and complex chiral amine architectures by embedding nitrogen motifs into the natural product precursors (Fig. 1D, top left) (22). Second, a commodity chemical, α-methylstyrene, could be applied as an N-methylation reagent (Fig. 1D, top right; for comparison with other N-methylation reagents, see section 4.5 of the supplementary materials) (23). Third, such a tool could facilitate the generation of useful value-added compounds that have been challenging to form or inaccessible from readily available starting materials. One such example is (1R,2R,5R)-5-amino-2-methylcyclohexan-1-ol hydrogen chloride, a precursor of a c-Jun N-terminal kinase (JNK) inhibitor. The considerable step economy and cost savings from previous approaches indicate the potential utility of this $C(sp^3)$–$C(sp^2)$ amination strategy in bioactive reagent synthesis (Fig. 1D, bottom) (24).

To accomplish the conversion of alkene $C(sp^3)$–$C(sp^2)$ σ bonds to $C(sp^3)$–N bonds, we had to address a fundamental challenge: cleavage of a stronger alkene $C(sp^3)$–$C(sp^2)$ σ bond [bond dissociation energy (BDE) = 102 kcal/mol for propene] preferably over an aliphatic alkyl $C(sp^3)$–$C(sp^3)$ σ bond (90 kcal/mol in ethane) (25). To realize this, our strategy engaged ozone, widely applied in several industries, to activate alkenes and facilitate their $C(sp^3)$–$C(sp^2)$ σ bond cleavages (26, 27). Ozonolysis of alkenes in alcoholic solvents affords α-alkoxyhydroperoxides via the Criegee intermediate (28). The weakness of the O–O bond (44 to 46 kcal/mol for alkyl hydroperoxides) of an α-alkoxyhydroperoxide can serve as the energetic driving force to promote fragmentation of the robust C–C bond. Previously, we had used Fe(II) salts as single-electron reducing agents to instigate O–O scission. The resulting α-alkoxyalkoxyl radical undergoes β-scission to release an alkyl radical that can be captured by organic radicophiles to provide the functionalization products of seemingly inert $C(sp^3)$–$C(sp^2)$ σ bonds (Fig. 1C, bottom) (29–31).

Copper is a redox-active metal that has been used for single-electron reduction of peroxide intermediates in both biological processes and synthetic chemistry (32). Recent studies have demonstrated that copper catalysts are efficient at trapping alkyl radicals to afford $C(sp^3)$–N bonds as reductive elimination products (12, 13, 33–36). We envisioned sequential reduction of the hydroperoxide intermediate by a copper(I) amido complex and trapping of the resultant alkyl radical by the copper(II) center to induce reductive elimination and, thereby, form the $C(sp^3)$–N bond in an overall redox-neutral process (Fig. 1C, bottom).

Reaction development

To implement our design, we investigated the impact of the copper salt, ligand, and solvent. We discovered that the aminodealkenylation could be performed efficiently under mild reaction conditions when using CuCl (20 mol %) and 1,10-phenanthroline (20 mol %) in acetonitrile (MeCN) at room temperature (see the supplementary materials for details). After determining the reaction conditions, we assessed a diverse array of nitrogen nucleophiles

for dealkenylative C–N coupling with (−)-isopulegol as the model alkene substrate (Fig. 2). Our protocol could be used to install functionalized indoles (**1** to **7**) into (−)-isopulegol in high yields, producing enantiomerically pure indole derivatives that are promising scaffolds for drug development (37). Two indole-based natural products, the sleep hormone melatonin (**6**) and a protected form of the amino acid tryptophan (**7**), were alkylated in high yields with exclusive regioselectivity in the presence of secondary amide N–H bonds. Other pharmaceutically important substituted heterocyclic compounds, including azaindoles (**8** to **10**), indazoles (**11** and **12**), carbazole (13), pyrazoles (**14** and **15**), and pyrrole (16), were successfully coupled with (−)-isopulegol in good yields. 6-Chloro-7-iodo-7-deazapurine (**17**), a privileged scaffold in anti-tumor and antiviral drugs, was also a competent alkylation substrate. We obtained high yields when coupling it with phthalimide (**18**), and this process could be scaled (50 mmol) with a slightly decreased yield. In addition to azacycles, we found that 2-aminopyrimidine (**19**), substituted anilines (**20** and **21**), and 2-aminopyridine (**22**) also underwent the dealkenylative C–N coupling efficiently. Less-nucleophilic amide (**23**) and sulfonamide (**24**) substrates also provided their coupling products in good yields. Notably, aryl halides were unaffected under the reaction conditions and might be used as functional handles for further derivatization.

To demonstrate the utility of this protocol in drug discovery, we applied our dealkenylative C–N coupling strategy to the late-stage functionalization of complex bioactive molecules. An *N*-tosyl prolinamide (**25**) and a dexibuprofen amide (**26**) were decorated with chiral 2-hydroxy-4-methylcyclohexyl groups in good yields. Two known pharmaceuticals, the non-steroidal anti-inflammatory celecoxib (**27**) and the antiretroviral lamivudine (**28**), were also N-alkylated effectively. Encouraged by the exclusive alkylation of the indole nitrogen atom of tryptophan, we explored the potential for indole N-functionalization of the tryptophan residue in the context of peptides featuring several amide N–H bonds. Both the tripeptide **29** and an endogenous opioid neurotransmitter, the endomorphin precursor **30**, underwent the site-selective C–N couplings in good yields with gentle heating. We also tested aliphatic amines, including benzylamine, dibenzylamine, and 1-phenylpiperazine, but none of them afforded desired C–N coupling products. We surmise that aliphatic amines serve as strongly donating ligands on copper, thereby influencing the coordination structures and redox potentials of the copper complexes **91** and **92**, in turn leading to inefficient regeneration of copper(I) species (see mechanistic studies and section 10.1 of the supplementary materials for details).

Scope of alkenes

Beyond (−)-isopulegol, we subjected an array of terpenes, terpenoids, and their derivatives to our deconstructive C–N coupling protocol to afford various artificial terpenoid alkaloids (Fig. 3). Most of these substrates are single enantiomers derived from natural products or are natural products themselves. (+)-Nootkatone and a eudesmane-type sesquiterpenoid underwent fragmentative C–N couplings with 3-chloroindazole and phthalimide to give the products **31a** and **31b** or **32a** and **32b**, respectively, in good yields with excellent diastereoselectivities. The bridged cyclic ketoester **33** was obtained in moderate yield and diastereoselectivity from the synthetic intermediate leading to (+)-seychellene. Although

good yields could be obtained regardless of substrate, the diastereoselectivity varied widely, especially when engaging the monocyclic terpenoids (−)-limonene-1,2-diol, (+)-dihydrocarvone ethylene glycol acetal, *cis*-(+)-limonene oxide, (+)-dihydrocarveol, (−)-perillyl alcohol oxide, (−)-carveol oxide, and (−)-*O*-benzoyl isopulegol (**34** to **40**). The observed diastereoselectivities are consistent with stereoselectivity trends commonly encountered in reactions with cyclic radicals, in which the stereoselectivity of the addition is dictated by a combination of torsional and steric effects (38, 39). All of the diastereoisomers [except two: the diastereoisomers of the minor regioisomers, **57a** and **57b**, from the aminodealkenylation of (−)-β-pinene] were separable through silica-column flash chromatography—a particularly relevant feature for lead compound discovery because diastereoisomers often exhibit drastically different bioactivities. Simple cyclohexyl and 4-piperidinyl radicals worked well when applied to the functionalization of melatonin (41) and tryptophan (42), respectively. We evaluated substrates bearing gem-disubstituted olefins, beyond the isopropenyl group, in the reaction and found that they provided primary alkyl-substituted amines in a facile manner (**43** to **47**). The epoxy indazole **43** was obtained in 83% yield from a (±)-α-ionone oxide derivative. A (−)-sclareol–derived alkene underwent smooth dealkenylative amination with 3-chloroindazole to afford the drimane meroterpenoid derivative **44** in 61% yield. Drimane meroterpenoids have diverse bioactivities, and our protocol provides a strategy toward N-heterocycles substituted with these terpenoid analogs (40). We used (*R*)-2,4-dimethylpent-4-en-1-ol, which can be accessed readily from Evans' auxiliary (~$3/g for *R*- or *S*-enantiomer) and 2-methallyl chloride, to synthesize (*R*)-3-(3-chloroindazolyl)-2-methylpropanol *O*-acetate (**45**), a precursor of muscarinic agonists, in 74% yield (41). Enantiopure 3-indazolyl-2-methylpropanols appear in 22 international patents and two US patents and were prepared from the corresponding (+)- and (−)-3-bromo-2-methyl-1-propanols (~$190/g from Sigma-Aldrich), which have previously been prepared from camphor sulfonic acids in five synthetic steps (42). Primary alkyl radicals from functionalized alkenes underwent efficient amination (**46** and **47**).

Monosubstituted alkenes were also competent substrates for our Cu-catalyzed dealkenylative C–N coupling (R = R′ = H); in contrast, these alkenes performed only moderately in Fe(II)-mediated dealkenylative radical couplings (29). We obtained a 73% isolated yield of the dealkenylative C–N coupling product **48** from (±)-dihydromyrcenol. Monosubstituted alkenes derived from (−)-β- citronellol and (+)-geraniol oxide *O*-acetate derivatives afforded the fragmented C–N coupling products **49a**, **49b**, and **50** in good yields. 1-Decene, which is produced from the Ziegler process or through cracking in the petroleum industry, worked well as a substrate to generate 3-chloro-1-octylindazole (**51**) in 67% yield. We found that an alkyl bromide, which could serve as a radical precursor, was tolerated under our conditions to produce *N*-(4-bromobutyl)phthalimide (**52**) in 55% yield. We also applied our deconstructive C–N coupling protocol to the modification of molecules of interest to materials science. The vinyl groups of chiral molecules used in liquid crystals were replaced by 3-chloroindazole in good yields (**53** and **54**). Another natural product, phytol, containing a trisubstituted alkene unit, underwent regioselective $C(sp^3)$–$C(sp^2)$ σ bond cleavage to afford the coupling products **55a** and **55b** in good yields. Compounds **55a** and **55b** could be considered azacycle analogs of vitamin E, where the benzopyran unit is substituted by chloroindazole and phthalimide moieties, respectively.

Alkylidenecycloalkanes were also suitable substrates for the dealkenylative C–N coupling process. (−)-β-Pinene provided the synthetically valuable chiral cyclobutanes **56a** and **57a** or **56b** and **57b** as 1.7:1 and 2.9:1 mixtures of regioisomers, respectively. In contrast, (±)-sabinene afforded the cyclopropane **58** as a single regioisomer in 78% yield. Methylene-adamantane (**59**) provided the equatorial amination product **60** exclusively. The β-amino acid derivative **62** was formed smoothly from the corresponding 4-methylenepiperidine **61**. The copper-catalyzed amination also converted the trisubstituted alkene **63** into the corresponding dealkenylated C–N coupling product **64** in 88% yield.

Chiral primary amine synthesis and its application

The ability to use aminodealkenylation to install phthalimide units into chiral-pool molecules provided an opportunity to synthesize chiral primary amines (Fig. 4). For example, we prepared the primary amine **65** in 75% yield from the phytol-derived phthalimide **55b**. Chiral amino alcohols are common in nature, and such bioactive compounds often serve as auxiliaries in organic synthesis. 1,2-Aminocyclohexanol is an important motif in organic synthesis and medicinal chemistry; we prepared its unusual 5-methylated analog **66** in 79% yield upon hydrazine-mediated deprotection of the phthalimide **18**. Similarly, we synthesized the aminocyclohexandiol **67** from the opposite enantiomer of **34b** (major diastereoisomer). Although 5-amino-3-methylpentan-1-ol is a useful building block, no asymmetric synthesis has been reported previously, and its racemic form costs $965.90/g. We obtained (*R*)-**68** upon deprotection of the phthalimide **49b** derived from (−)-β-citronellol. The chiral amino acid ester **69** can be synthesized from (−)-β-pinene. The abundant functional groups in terpenoids also facilitated the synthesis of more-elaborate amino alcohols through diversification. For example, we prepared the amino alcohol **71** from *cis*-(−)-limonene oxide through aminodealkenylation, thiolation, and deprotection. We obtained the amino alcohol **73**, bearing a nootkatol skeleton, through the Luche reduction of **31b**, followed by deprotection. We synthesized the artificial indole alkaloid **75** through sequential Fischer indolization of **32b** with 4-methoxylphenylhydrazine and deprotection. (1*R*,2*R*,5*R*)-5-Amino-2-methylcyclohexanol (**77**) is a synthetic intermediate leading to a JNK inhibitor (Fig. 1D) (24, 43); previous routes to its synthesis have involved 12 steps from (−)-limonene and 11 steps from the Diels-Alder reaction of isoprene and methyl acrylate. Using our deconstructive C–N coupling strategy with commercially available (−)-dihydrocarveol ($3.10/g) and phthalimide, followed by deprotection using hydrazine monohydrate, afforded **77** in two steps in 54% overall yield. Chiral 4-substituted-1-methylcyclohexenes are synthetically challenging molecules and serve as key intermediates in the synthesis of various pharmaceuticals and natural products (44). (*S*)-1-Methylcyclohexenyl-4-amine (**79**, $1930.50/g) has been a precursor in the synthesis of a trichodiene synthase inhibitor. The previous route to **79** involved eight steps from chiral limonenes (45). The enantioenriched phthalimide **78** was prepared recently by Liu and co-workers in four steps, including an alkene desymmetrization strategy using a chiral cobalt (II) complex catalyst, which was prepared in six steps from L-alaninol (44). Our strategy engaged commercially available *cis*-(−)-limonene oxide for dealkenylative amination, in which the C–N coupling products were produced in 83% yield with 2.1:1 diastereomeric ratio (d.r.), with the desired diastereoisomer (isolated in 56%

yield), after subsequent deoxygenation, affording the chiral phthalimide **78** in 55% yield. The deprotection proceeded smoothly to afford the primary amine **79** in 85% yield (29% overall yield over three steps). Considering the capability of copper-catalyzed coupling with various nucleophiles, our strategy might provide facile access to chiral 4-substituted-1-methylcyclohexenes.

Methylation reactions

α-Methylstyrene (AMS), a by-product of the cumene process, is produced in quantities of >292,000 tons annually (46). Because of the relative stability of the methyl radical (BDE: 105.0 kcal/mol for Me–H) over the phenyl radical (BDE: 112.9 kcal/mol for Ph–H) (25), we surmised that the Criegee ozonolysis product of AMS, upon exposure to the Cu(I) complex, should produce methyl radicals and, thereby, methylated amines (23). Indeed, we found that reactions with AMS readily generated 1-methyl-3-chloroindazole (**80**) and caffeine (from theophylline) under our protocol, in yields of 84 and 67%, respectively. We methylated zidovudine, an anti-HIV drug, at the N3 atom of the thymidine moiety to afford 3-methylzidovudine, without protecting the 5′-hydroxyl group. Particularly useful methylations were those of canonical nucleosides. N^6-Methyladenosine (**m⁶A**) is the most abundantly modified nucleoside in eukaryotic mRNAs; it plays a crucial role in controlling gene expression in cellular, developmental, and disease processes (47). When using our protocol, adenosine ($0.097/g) can be methylated directly to **m⁶A** ($103.40/g) in 72% isolated yield in a single step, compared with the two or three steps in previous reports. We achieved another common RNA modification, **m^{6,6}A** ($148/g), in nearly quantitative yield when using an additional equivalent of AMS (compared with the two steps in a previous report). We also performed the reaction on a 5-g scale, providing a pure sample without the need for silica-column purification. We used the deuterium-labeled α-trideuteromethylstyrene (**81**), obtained from acetophenone and deuterium oxide in two steps, to generate isotopically labeled **D₃-m⁶A** ($7030/g). We prepared other common methylated nucleosides, namely **m⁶dA** ($510/g), **m⁴C** ($420/g), and **m⁴dC** ($16.70/mg), from the corresponding canonical deoxyadenosine, cytidine, and deoxycytidine, respectively, in good yields, where multiple synthetic steps or low yields were previously necessary (see the supplementary materials for previous routes).

Terpene nucleosides

Encouraged by the successful nucleoside methylation, we used aminodealkenylation for the rapid construction of terpene nucleosides (Fig. 4C). Terpene nucleoside natural products are generated through the adenosine processing of sesquiterpenoids or diterpenoids. They are found in bacterial metabolites and exhibit considerable biofunctionality and bioactivity —for example, as an antacid signaling molecule or as a component in the cell wall of *Mycobacterium tuberculosis* (48). Furthermore, an adenosine-processed eudesmane-type sesquiterpenoid isolated from the myxobacterium *Sorangium cellulosum* exhibited moderate anti-bacterial activity against a wide range of bacterial strains (49). We used the eudesmane-type sesquiterpenoid (**82**), (+)-nootkatone (**83**), drimane sesquiterpenoid (**84**), and the monoterpene (−)-isopulegol (**85**) to prepare terpene nucleosides in moderate to good yields. Analogs of terpene nucleosides can be applied as chemical probes of biological function,

and their innate bioactivity might also provide a platform for developing lead compounds in medicinal research.

Mechanistic studies

We conducted several experiments to gain insight into the reaction mechanism. Copper halides and phenanthroline are known to form tight ion pairs [(Phen)$_2$Cu]$^+$[CuX$_2$]$^-$ instead of neutral complexes [(Phen)CuX] in polar solvents (50, 51), and our ultraviolet–visible spectroscopic measurements indicated that the ion pair complex [(Phen)$_2$Cu]$^+$[CuCl$_2$]$^-$ was the dominant species in MeCN (see the supplementary materials for details). Previous mechanistic studies have suggested that the neutral complex is the active species in the C–N coupling reaction, due to inefficient oxidative addition of ionic copper complexes to aryl halides (17, 51). In contrast to oxidative addition, single-electron transfer (SET) between hydroperoxide and either [(Phen)$_2$Cu]$^+$ or [CuCl$_2$]$^-$ is rapid [the rate constant (k) $\approx 4 \times 10^3$ M^{-1} s^{-1}] and can trigger peroxide fragmentation (52, 53).

In an attempt to directly probe the nature of the reactive copper species, we prepared a series of copper complexes (Fig. 5A) and compared their performance in the aminodealkenylation between (−)-dihydrocarveol and phthalimide. When the prototypical mixture of 1:1 CuCl and phenanthroline was replaced with a neutral phthalimido copper complex {[(Phen)Cu(phth)] (**86**) or [(Phen)Cu(phth)$_2$] (**87**)}, which had been proposed previously as a reactive intermediate (15, 17), both the product yields (45 and 44%, respectively) and diastereoisomeric ratios (1.8:1.0 and 1.4:1.0, respectively) deteriorated substantially when compared with those of the standard reaction (90% nuclear magnetic resonance yield, 2.9:1.0 d.r.) (entries 1 to 3). Using the ion pair [(Phen)$_2$Cu]$^+$ [CuCl$_2$]$^-$ (**88**) directly afforded a reaction similar to the prototypical aminodealkenylation (87% yield, 2.8:1.0 d.r.), indicating that the ion pair might have been the active catalytic species. Reactions using either [(Phen)$_2$Cu]$^+$ (**89**) or [CuCl$_2$]$^-$ (CuCl + Et$_4$NCl) were extremely sluggish (entries 5 and 6), whereas the combination of independently prepared [(Phen)$_2$Cu]$^+$ and [CuCl$_2$]$^-$ afforded a product similar to that from the parent reaction (entries 4 and 7), but with a slightly diminished yield.

To gain further insight into the mechanism of the copper-catalyzed amination, we conducted kinetic studies through variable time normalization analysis (VTNA) (54). Using ReactIR, we collected the concentration–time profiles for both the C–C scission product [methyl acetate (MeOAc)] and the C–N coupling product (**32b**). The formation of MeOAc displayed 0.3-, zero-, and 1.3-order dependences with respect to **S32-peroxide**, phthalimide, and the catalyst (CuCl + Phen), respectively, while the coupling product **32b** displayed 0.3-, 0.3-, and 1.3-order dependences (figs. S22 to S27). The zero– and pseudo-zero–order dependences on both peroxide and the amine imply that there existed an off-cycle catalyst resting state (55, 56). Because both [(Phen)$_2$Cu]$^+$ and [CuCl$_2$]$^-$ are readily oxidized by peroxide, we surmise that the resting states of the catalyst were the corresponding copper(II) species **91** and **93** (Fig. 5C, reactions 1 to 3). The kinetic order of 1.3 with respect to catalyst indicates a scenario in which two catalytic species were operating on-cycle (Fig. 5C).

To tease out the roles of the cation and anion complexes in the catalytic cycle, we investigated the kinetics of $[(Phen)_2Cu]^+$ (**89**) and $[CuCl_2]^-$ (1:1 mixture of CuCl + Et$_4$NCl) separately. Both the C–C scission and C–N coupling events exhibited a kinetic order of 1.3 in $[CuCl_2]^-$ in the presence of 2 mol % **89** (Fig. 5B, i and ii, and figs. S32 and S33) and a kinetic order of 2 in the presence of 0.5 mol % **89** (figs. S34 and S35). Moreover, although $[CuCl_2]^-$ alone could catalyze the generation of MeOAc (Fig. 5B, iii), the formation of **32b** was sluggish in the absence of $[(Phen)_2Cu]^+$ (Fig. 5B, iv, and Fig. 5A, entry 6). In sum, the C–C scission and C–N coupling steps displayed zero-and first-order dependences on $[(Phen)_2Cu]^+$ at low concentrations (0.1 to 0.5 mmol %; Fig. 5B, iii and v) and saturation kinetics at higher concentrations (0.5 to 2.0 mol %), respectively, each in the presence of 2.0 mol % $[CuCl_2]^-$ (figs. S28 to S31). The amount of **89** did not affect C–C scission, generating MeOAc even in its absence (Fig. 5B, iii), while both the production rate and yield of **32b** were dependent on the concentration of **89** (Fig. 5B, iv). Complex **89** alone, however, could not generate appreciable amounts of MeOAc and **32b**, both of which were generated steadily upon addition of Et$_4$NCl (Fig. 5B, vi). We surmise that $[(Phen)_2Cu]^{2+}$ (**93**) was a stable cation whose reduction back to Cu(I) species was sluggish. Therefore, once $[(Phen)_2Cu]^+$ was oxidized, the reaction stalled (Fig. 5C, reaction 3). Nevertheless, the addition of chloride replenished some Cu(II)Cl$_m$L$_n$ species that could oxidize the peroxide **A** and the radical **B** and return to the Cu(I) species (Fig. 5C, reactions 1 and 2) (57). The disparate reaction kinetics of $[CuCl_2]^-$ and $[(Phen)_2Cu]^+$ indicate that $[CuCl_2]^-$ was involved in hydroperoxide decomposition, whereas $[(Phen)_2Cu]^+$ participated in the C–N coupling. Because C–C scission occurred before C–N coupling, $[CuCl_2]^-$ influenced both the C–C scission and C–N coupling processes (figs. S34 and S35).

Taken together, we propose the involvement of $[CuCl_2]^- - [(Phen)_2Cu]^+$ cooperative catalysis (Fig. 5C). SET between complex **90** and the peroxide **A** affords the alkoxyl radical **E**, which undergoes β-scission to generate the alkyl radical **B**. The cationic Cu(I) complex **92** is oxidized by peroxide **A** to afford a copper(II) complex **93**. Deprotonated phthalimide associates with complex **93**, followed by dissociation of Phen, to afford the phthalimido copper(II) complex **94**. Complex **94** traps the alkyl radical **B** to afford the C–N coupling product and the copper(I) complex **97** through either an outer sphere (**95**) or inner sphere (**96**) pathway (58). Ligand exchange on the Cu(I) complex **97** affords **92**. Subsequent electron transfer between **91** and **92** regenerates **90** and **93**, completing a catalytic cycle. Alternatively, electron transfer between **97** and **91** is also possible to regenerate **90**. Deprotonated phthalimide associates with the resulting Cu(II) complex from **97** to regenerate **94**, completing the catalytic cycle. Given the straightforward nature of the modular introduction of nitrogen moieties through the unusual disconnection of alkene skeletons, we anticipate that our copper-catalyzed dealkenylative C–N coupling will find applications in the preparation of complex bioactive three-dimensional molecules and optically active amines of great interest in organic synthesis and medicinal chemistry.

Supplementary Material

Refer to Web version on PubMed Central for supplementary material.

ACKNOWLEDGMENTS

Data and materials availability:

Experimental procedures, optimization data, and characterization data are available in the supplementary materials.

REFERENCES AND NOTES

1. Vitaku E, Smith DT, Njardarson JT, J. Med. Chem 57, 10257–10274 (2014). [PubMed: 25255204]

2. Brown DG, Boström J, J. Med. Chem 59, 4443–4458 (2016). [PubMed: 26571338]

3. Trowbridge A, Walton SM, Gaunt MJ, Chem. Rev 120, 2613–2692 (2020). [PubMed: 32064858]

4. Chen F, Wang T, Jiao N, Chem. Rev 114, 8613–8661 (2014). [PubMed: 25062400]

5. Xia Y, Dong G, Nat. Rev. Chem 4, 600–614 (2020). [PubMed: 34708156]

6. Roque JB, Kuroda Y, Göttemann LT, Sarpong R, Nature 564, 244–248 (2018). [PubMed: 30382193]

7. Tinge J et al., in Ullmann's Encyclopedia of Industrial Chemistry (Wiley, 2018), pp. 1–31.

8. Liu J et al., Nat. Chem 11, 71–77 (2019). [PubMed: 30374038]

9. Liu J et al., Science 367, 281–285 (2020). [PubMed: 31806697]

10. Liu J et al., Research 2020, 7947029 (2020). [PubMed: 33274339]

11. Zhao W, Wurz RP, Peters JC, Fu GC, J. Am. Chem. Soc 139, 12153–12156 (2017). [PubMed: 28841018]

12. Mao R, Frey A, Balon J, Hu X, Nat. Catal 1, 120–126 (2018).

13. Liang Y, Zhang X, MacMillan DWC, Nature 559, 83–88 (2018). [PubMed: 29925943]

14. Hu X et al., ACS Catal. 10, 8402–8408 (2020).

15. Lv X-Y, Abrams R, Martin R, Angew. Chem. Int. Ed 62, e202217386 (2023).

16. Chiusoli GP, Minisci F, Gazz. Chim. Ital 88, 261–270 (1958).

17. Tran BL, Li B, Driess M, Hartwig JF, J. Am. Chem. Soc 136, 2555–2563 (2014). [PubMed: 24405209]

18. Guo J-J et al., Angew. Chem. Int. Ed 55, 15319–15322 (2016).

19. Sakurai S, Kato T, Sakamoto R, Maruoka K, Tetrahedron 75, 172–179 (2019).

20. Bao J, Tian H, Yang P, Deng J, Gui J, Eur. J. Org. Chem 2020, 339–347 (2020).

21. Ertl P, Schuhmann T, J. Nat. Prod 82, 1258–1263 (2019). [PubMed: 30933507]

22. Nugent TC, Ed., Chiral Amine Synthesis: Methods, Developments and Applications (Wiley-VCH, 2010).

23. Ospina F et al., Angew. Chem. Int. Ed 61, e202213056 (2022).

24. Man H-W et al. , Solid forms of 2-(tert-butylamino)-4-((1R,3R,4R)-3-hydroxy-4-methylcyclohexylamino)-pyrimidine-5-carboxamide, compositions thereof and methods of their use, United States Patent US 9365524 B2, 14 June 2016.

25. Luo Y-R, Comprehensive Handbook of Chemical Bond Energies (CRC Press, 2007).

26. Fisher TJ, Dussault PH, Tetrahedron 73, 4233–4258 (2017).

27. Epelle EI et al., Chem. Eng. J 454, 140188 (2023). [PubMed: 36373160]

28. Criegee R, Wenner G, Justus Liebigs Ann. Chem 564, 9–15 (1949).

29. Smaligo AJ et al., Science 364, 681–685 (2019). [PubMed: 31097667]

30. Dworkin JH, Dehnert BD, Kwon O, Trends Chem. 5, 174–200 (2023). [PubMed: 38108020]

31. Dehnert BD, Dworkin JH, Kwon O, Synthesis (2023).

32. Trammell R, Rajabimoghadam K, Garcia-Bosch I, Chem. Rev 119, 2954–3031 (2019). [PubMed: 30698952]

33. Bissember AC, Lundgren RJ, Creutz SE, Peters JC, Fu GC, Angew. Chem. Int. Ed 52, 5129–5133 (2013).

34. Chen C, Peters JC, Fu GC, Nature 596, 250–256 (2021). [PubMed: 34182570]

35. Górski B, Barthelemy A-L, Douglas JJ, Juliá F, Leonori D, Nat. Catal 4, 623–630 (2021).

36. Dow NW, Cabré A, MacMillan DWC, Chem 7, 1827–1842 (2021). [PubMed: 34423174]

37. Sravanthi TV, Manju SL, Eur. J. Pharm. Sci 91, 1–10 (2016). [PubMed: 27237590]

38. Giese B, Angew. Chem. Int. Ed 28, 969–980 (1989).

39. Bar G, Parsons AF, Chem. Soc. Rev 32, 251–263 (2003). [PubMed: 14518178]

40. Dixon DD, Lockner JW, Zhou Q, Baran PS, J. Am. Chem. Soc 134, 8432–8435 (2012). [PubMed: 22583115]

41. Burstein ES et al. , Preparation of indazole compounds as muscarinic agonists, International Patent WO 2014/152144 Al, 25 September 2014.

42. Mekala S, Hahn RC, J. Org. Chem 80, 1610–1617 (2015). [PubMed: 25536280]

43. Connolly TJ, Man H-W, Nagarajan P, Rajendiran C, Venkateswarlu J, Methods of synthesis of (1R,2R,5R)-5-amino-2-methylcyclohexanol hydrochloride and intermediates useful therein, International Patent WO 2017/019487 A1, 2 February 2017.

44. Liu X, Rong X, Liu S, Lan Y, Liu Q, J. Am. Chem. Soc 143, 20633–20639 (2021). [PubMed: 34870975]

45. Cane DE, Yang G, Coates RM, Pyun HJ, Hohn TM, J. Org. Chem 57, 3454–3462 (1992).

46. The annual production volume of α-methylstyrene (AMS) was obtained at https://www.globenewswire.com/news-release/2019/05/27/1850397/0/en/542-9-Mn-Alpha-Methylstyrene-Market-Global-Forecast-to-2024.html. Please refer to the supplementary materials for its price as well as the price of each chemical in this study.

47. Zaccara S, Ries RJ, Jaffrey SR, Nat. Rev. Mol. Cell Biol 20, 608–624 (2019). [PubMed: 31520073]

48. Holzheimer M, Buter J, Minnaard AJ, Chem. Rev 121, 9554–9643 (2021). [PubMed: 34190544]

49. Ahn J-W, Jang KH, Chung S-C, Oh K-B, Shin J, Org. Lett 10, 1167–1169 (2008). [PubMed: 18288853]

50. Pallenberg AJ, Koenig KS, Barnhart DM, Inorg. Chem 34, 2833–2840 (1995).

51. Tye JW, Weng Z, Johns AM, Incarvito CD, Hartwig JF, J. Am. Chem. Soc 130, 9971–9983 (2008). [PubMed: 18597458]

52. Masarwa M et al., J. Am. Chem. Soc 110, 4293–4297 (1988).

53. Ponganis KV, De Araujo MA, Hodges HL, Inorg. Chem 19, 2704–2709 (1980).

54. Burés J, Angew. Chem. Int. Ed 55, 2028–2031 (2016).

55. Blackmond DG, J. Am. Chem. Soc 137, 10852–10866 (2015). [PubMed: 26285166]

56. Alamillo-Ferrer C, Hutchinson G, Burés J, Nat. Rev. Chem 7, 26–34 (2023). [PubMed: 37117826]

57. Moffett JW, Zika RG, Environ. Sci. Technol 21, 804–810 (1987). [PubMed: 19995065]

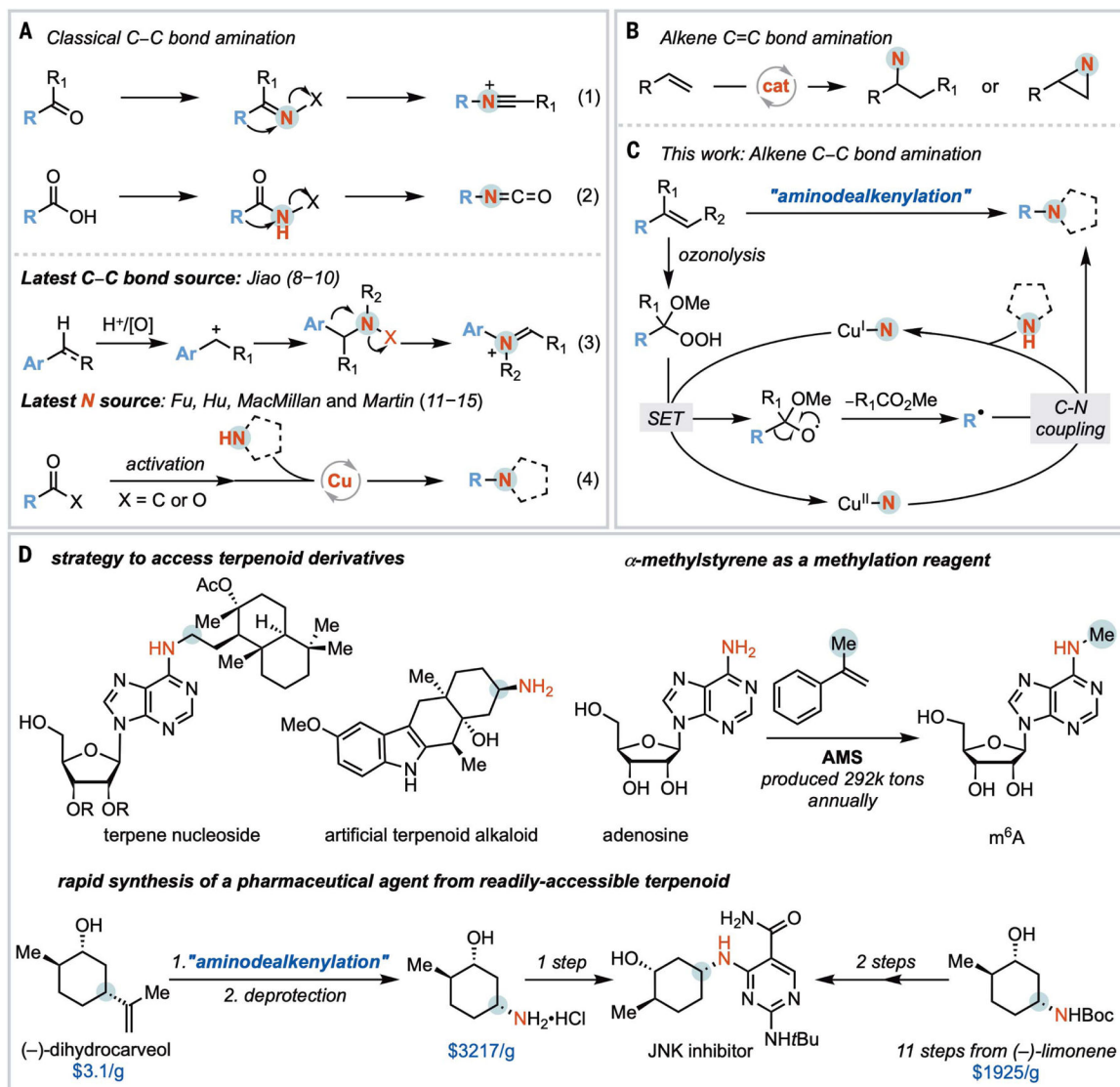58. Lee H et al., J. Am. Chem. Soc 144, 4114–4123 (2022). [PubMed: 35167268]

Fig. 1. Concept and development of dealkenylative C(sp³)–N bond coupling.
(**A**) Classic strategies in C(sp³)–N bond construction from carbonyl compounds and recent advances. (**B**) C(sp³)–N formation from alkene π bonds. (**C**) C(sp³)–N formation from alkene σ bonds. (**D**) Applications of dealkenylative C(sp³)–N bond coupling. SET, single-electron transfer; cat, catalysis; AcO, acetoxy; Me, methyl; *t*Bu, tert-butyl; Boc, *tert*-butoxycarbonyl.
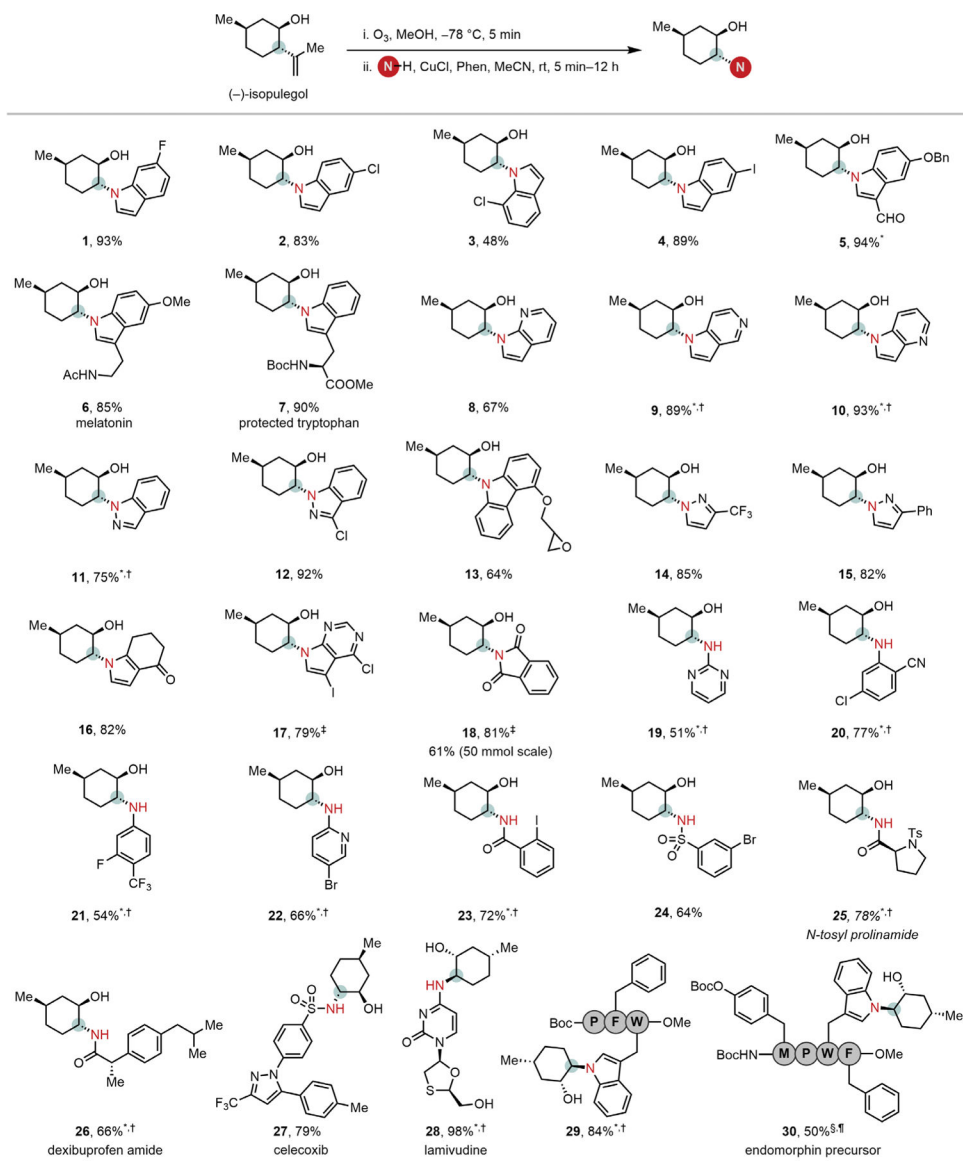
Fig. 2. Substrate scope of nitrogen nucleophiles.

Reactions were performed on a 0.2- to 2.0-mmol scale using 20 mol % CuCl and 20 mol % phenanthroline (Phen) at 23°C in MeCN. All yields are isolated yields. Absolute configurations are indicated by wedged and dashed bonds. *3 equiv of alkene was used. †30 mol % of CuCl and 30 mol % of Phen were used. ‡2.5 equiv of alkene was used. §5.0 equiv of alkene was used. ¶The reaction was performed at 60°C. OBn, benzyloxy; Ph, phenyl.
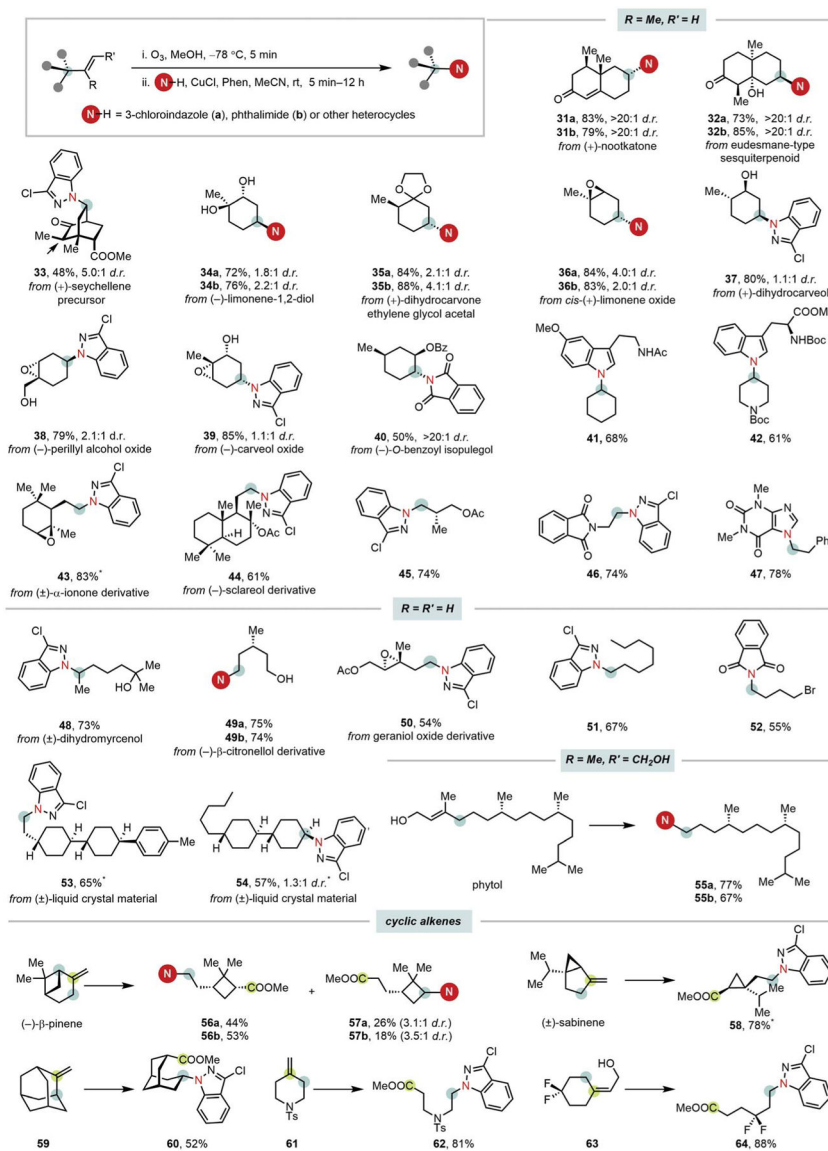
Fig. 3. Substrate scope of alkenes.
All yields are isolated yields. For the detailed reaction conditions of each substrate, see the supplementary materials. Absolute configurations are indicated by wedged or dashed bonds, unless otherwise specified. The diastereoisomers were separated by flash column chromatography; major diastereoisomers are shown. *Wedged and dashed bonds indicate the relative stereochemistry, because the racemic starting material was used.
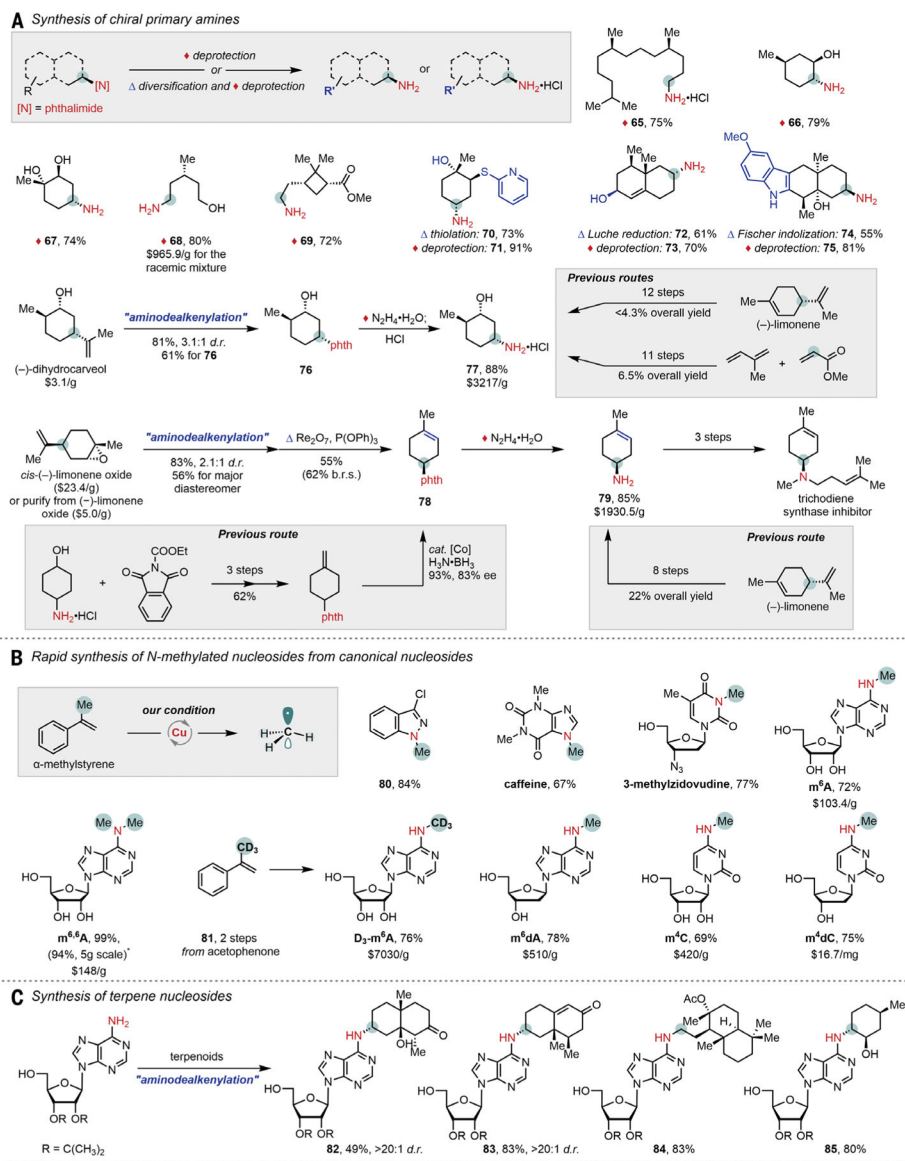
Fig. 4. Application of dealkenylative C(sp³)–N bond coupling in bioactive compound synthesis.
(**A**) Syntheses of complex chiral amines and bioactive compounds. (**B**) Methylation of nucleosides. (**C**) Terpene-nucleoside synthesis. *No flash column chromatography purification was necessary. b.r.s., base on recovered starting material; ee, enantiomeric excess.
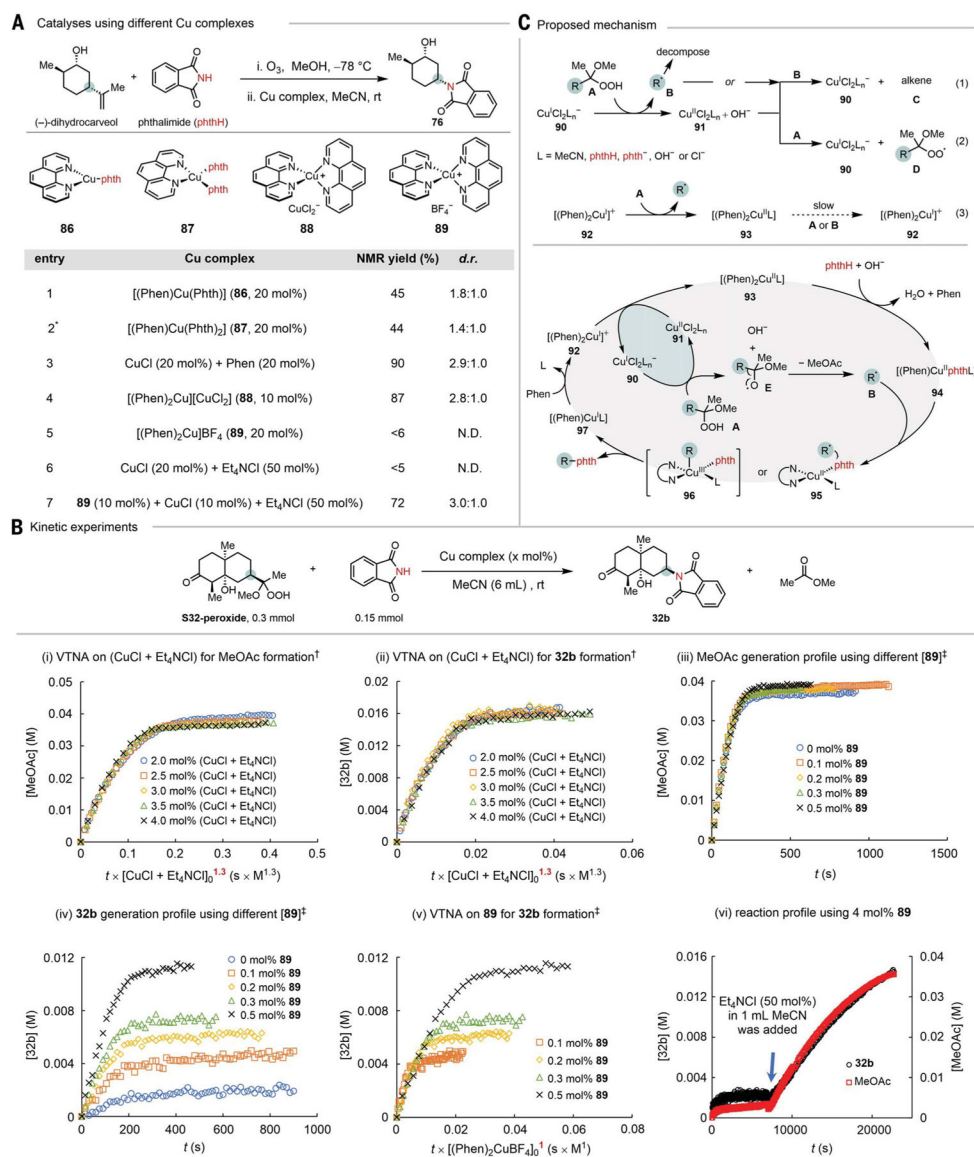
Fig. 5. Mechanistic studies.
(**A**) Comparison of different copper complexes. (**B**) Kinetic studies. (**C**) Proposed mechanism. *MeCN/MeOH (9:1 v/v) was used because complex **87** does not dissolve in MeCN. †2 mol % of **89** was used. ‡2 mol % of (CuCl + Et$_4$NCl) was used. N.D., not determined.